A Synthetic Peptide Blocking the Apolipoprotein E/β-Amyloid Binding Mitigates β-Amyloid Toxicity and Fibril Formation *in Vitro* and Reduces β-Amyloid Plaques in Transgenic Mice

Marcin Sadowski,* Joanna Pankiewicz,*
Henrieta Scholtzova,* James A. Ripellino,*
Yongsheng Li,* Stephen D. Schmidt,[†]
Paul M. Mathews,[†] John D. Fryer,[‡]
David M. Holtzman,[‡] Einar M. Sigurdsson,[§¶] and
Thomas Wisniewski*[§¶]

From the Departments of Neurology, Psychiatry[§] and
Pathology,[¶] New York University School of Medicine, New York,
New York; Nathan S. Kline Institute,[†] New York University,
Orangeburg, New York; and the Departments of Neurology,
Molecular Biology, and Pharmacology,[‡] Center for the Study of
Nervous System Injury, Washington University School of
Medicine, St. Louis, Missouri*

Alzheimer's disease (AD) is associated with accumulation of β-amyloid (Aβ). A major genetic risk factor for sporadic AD is inheritance of the apolipoprotein (apo) E4 allele. ApoE can act as a pathological chaperone of Aβ, promoting its conformational transformation from soluble Aβ into toxic aggregates. We determined if blocking the apoE/Aβ interaction reduces Aβ load in transgenic (Tg) AD mice. The binding site of apoE on Aβ corresponds to residues 12 to 28. To block binding, we synthesized a peptide containing these residues, but substituted valine at position 18 to proline (Aβ12–28P). This changed the peptide's properties, making it non-fibrillogenic and non-toxic. Aβ12–28P competitively blocks binding of full-length Aβ to apoE (IC$_{50}$ = 36.7 nmol). Furthermore, Aβ12–28P reduces Aβ fibrillogenesis in the presence of apoE, and Aβ/apoE toxicity in cell culture. Aβ12–28P is blood-brain barrier-permeable and in AD Tg mice inhibits Aβ deposition. Tg mice treated with Aβ12–28P for 1 month had a 63.3% reduction in Aβ load in the cortex (P = 0.0043) and a 59.5% (P = 0.0087) reduction in the hippocampus comparing to age-matched control Tg mice. Antibodies against Aβ were not detected in sera of treated mice; therefore the observed therapeutic effect of Aβ12–28P cannot be attributed to an antibody clearance response. Our experiments demonstrate that compounds blocking the interaction between Aβ and its pathological chaperones may be beneficial for treatment of β-amyloid deposition in AD. *(Am J Pathol 2004, 165:937–948)*

A disturbance of amyloid-β (Aβ) homeostasis in Alzheimer's disease (AD) leads to the accumulation of this peptide in the form of plaques in the brain.[1] Increased production of Aβ peptides or their inadequate clearance can lead to brain accumulation. It has been demonstrated that peptides homologous to Aβ form amyloid fibrils in solution if they reach a critical concentration.[2] This process can be effectively promoted by Aβ pathological chaperone proteins (for review, see[3]) such as apolipoprotein E (apoE), especially its E4 isoform,[4] ∝ 1-antichymotrypsin (ACT),[5] or C1q complement factor.[6] They promote formation of Aβ fibrils, which remain sequestered within the brain and accumulate in the form of plaques.[7] Inheritance of the apo E4 isoform has been identified as the major identified genetic risk factor for sporadic, late-onset AD[8] and correlates with an earlier age of onset and greater Aβ deposition, in an allele dose-dependent manner.[8–10] ApoE is a 34-kd glycosylated protein existing in three major isoforms E2, E3, and E4, which differ in primary sequence at two residues. The chaperoning effect of apo E on the formation of Aβ deposits has been studied in great detail. *In vitro*, all apo E isoforms can propagate the β-sheet content of Aβ peptides promoting fibril formation,[11] with apo E4 being the most efficient.[4] The dependence of Aβ deposition in plaques on the presence of apoE has also been confirmed *in vivo*. Crossing APP^{V717F} AD transgenic (Tg) mice onto an apoE knockout (KO) background resulted in a substantial reduction of the Aβ load and an absence of fibrillar Aβ deposits.[12] Therefore, one can speculate that the selective ablation of apoE's effect on Aβ could potentially have a therapeutic effect leading to diminished Aβ deposition and decreased Aβ toxicity. ApoE hydro-

phobically binds Aβ, forming SDS insoluble complexes.[13–15] Although the affinity of binding depends on Aβ conformation (Aβ soluble *versus* fibrillar), it remains in the low nanomolar range.[11,13,16,17] Prior studies have identified that residues 12–28 of Aβ are the binding site for apoE on Aβ.[13,18] This sequence encompasses a hydrophobic domain (residues 14–21) and a β-turn (residues 22–28) which place two hydrophobic domains of Aβ (14–21 and 29–40/42) opposite each other allowing for assembly of Aβ peptides into fibrils.[19] Ma et al[20] have demonstrated that a synthetic peptide homologous to 12–28 amino acid sequence of Aβ can be used as a competitive inhibitor of the binding of full-length Aβ to apo E, resulting in reduced fibril formation and increased survival of cultured neurons. These *in vitro* studies confirmed that the interaction of apoE with residues 12–28 of Aβ is not just a non-specific hydrophobic interaction but plays a pivotal role in the mechanism of Aβ pathology in AD. The goal of this study is to investigate whether compounds blocking the apoE/Aβ interaction can be developed into a novel therapeutic approach for AD. Aβ12–28 can be associated with toxicity, due to the 14 to 21 residue hydrophobic domain.[21] It can also co-deposit on existing Aβ plaques when injected into AD transgenic (Tg) mice.[22] Therefore, we have modified the Aβ12–28 sequence by substitution of the valine at residue 18 to proline, rendering this peptide non-fibrillogenic and non-toxic. Use of D-amino acids, amidation of the C-terminus, and acetylation of the N-terminus were designed to extend the serum half-life of the peptide, prolonging *in vivo* activity. In a series of experiments we analyzed the effect of pharmacological blockade of apo E's pathological chaperoning properties on Aβ fibrillogenesis and toxicity *in vitro* using Aβ12–28 and Aβ12–28P. Aβ12–28P was also administered to AD Tg mice to investigate the *in vivo* effect of blocking the apoE/Aβ interaction on Aβ deposition.

Materials and Methods

Synthetic Peptides and Proteins

Aβ1–40, Aβ1–42, Aβ12–28, and Aβ12–28P were synthesized in the W. M. Keck Facility at Yale University. Details of synthesis, purification, and sequence verification were described previously.[23–25] Aβ12–28P (VHHQKLPFFAED-VGSNK) was synthesized using D-amino acids and end protected by amidation of the C-terminus and acetylation of the N-terminus to minimize degradation by endogenous peptidases and extend the half-life. Aβ12–28 (VH-HQKLVFFAEDVGSNK) used in fibrillization and tissue culture assays was also synthesized using D-amino acids to control for the racemic isomer effect. For aggregation studies and assessment of secondary structure, the peptides were treated with 1,1,1,3,3,3-hexafluoro-2-propanol (HFIP; Sigma, St. Louis, MO) as described elsewhere.[26] This treatment renders peptides monomeric with minimal β-sheet content.

Recombinant apo E3 and apo E4, were purchased from Calbiochem Corp. (San Diego, CA). Lipidated apo E3 and apo E4 complexes were prepared from primary cultures of astrocytes derived from Tg mice in which human apo E3 or apo E4 were expressed under the control of the astrocyte-specific glial fibrillary acidic protein (GFAP) promoter as described previously.[27–29] Briefly, primary cultures of forebrain astrocytes were maintained in serum-free Dulbecco's modified Eagle's medium/Ham's F-12 (1:1) with N2 supplement (Invitrogen, Carlsbad, CA) for 72 hours. The medium was removed and clarified by centrifugation at $800 \times g$ for 5 minutes and then concentrated by ultra-filtration. Human apoE was isolated by immunoaffinity chromatography. The purity of the apoE preparation was assessed by SDS-PAGE.[28]

Circular Dichroism Studies of Secondary Structure

Aliquots of HFIP-treated peptides were reconstituted in 5 mmol/L Tris buffer (pH 7.0) to obtain a peptide concentration of 100 μmol/L and were incubated at 37°C. Circular dichroism (CD) was measured at indicated intervals with t = 0 being immediately after the peptide was reconstituted on a Jasco J-720 spectropolarimeter (Jasco, Inc., Easton, MD) equipped with a model CTC-344 circular temperature control system (Neslab Inc., Newington, NH) according to our previously described protocols.[11,30,31] The Lincomb, convex constraints and neural network algorithms (Softsec software; Softwood Inc., Scranton, PA) were used to obtain percentages of different types of secondary structures of analyzed peptides.[32–35]

Aggregation and Fluorometric Experiments

All peptides were incubated alone at concentrations 100 μmol/L over a period of 10 days at 37°C in 100 mmol/L Tris buffer (pH 7.4). Aβ1–42 was also incubated in the presence of 1μmol/L of lipidated apo E3 or E4 (100:1 molar ratio). In aggregation inhibition experiments, apo E3 or E4 was preincubated with Aβ12–28P in a molar ratio of 1:2 for 6 hours at 37°C and then added to freshly reconstituted Aβ1–42. Aβ1–42 was incubated with Aβ12–28P at a molar ratio of 100:2 as a control. Amount of fibrils formed by the different peptides at different time points was evaluated by a Thioflavin-T assay on a Perkin-Elmer LS-50B fluorescence spectrophotometer (Perkin Elmer Instruments, Shelton, CT) according to previously published methods.[4,11] The mean ± SD (SD) for three separate experiments was plotted in Figure 1. Statistical analysis was performed by means of a repeated measures analysis of variance followed by a Tukey HSD post-hoc test using CSS Statistica (version 6.1, StatSoft Inc.; OK).

Cell Culture Neurotoxicity Studies

The effect of 1 to 100 μmol/L concentrations of Aβ12–28 and Aβ12–28P on the viability of the SK-N-SH human neuroblastoma cell line (American Type Culture Collection, Manassas, VA) was compared to the well estab-

lished neurotoxicity of Aβ1–40 and Aβ1–42 in this cell line model.[24,36,37] Viability of SK-N-SH cells cultured in a flat-bottom, 96-well microtiter plates in the presence of peptides for 2 days, was assessed using the (3-(4,5-dimethylthiazol-2yl)-2,5-diphenyl tetrasodium (MTT) metabolic assay[20] according to the manufacturer's manual (Roche Molecular Biochemicals, Indianapolis, IN).

In toxicity rescue experiments Aβ12–28 or Aβ12–28P were used to neutralize lipidated apoE4's effect on Aβ1–42 neurotoxicity. Aβ12–28 or Aβ12–28P was preincubated with apo E4 in an equimolar concentration for 6 hours at 37°C then mixed with Aβ1–42, followed by addition to microtiter plates containing SK-N-SH cells. For comparison, cells were incubated with Aβ1–42 alone and with Aβ1–42 and apoE4. Apo E alone, Aβ1–42+Aβ12–28 and Aβ1–42+Aβ12–28P were used as additional controls. The final concentration of peptides was as follows: Aβ1–42 100 μmol/L, Aβ12–28 and Aβ12–28P 0.5 μmol/L and apoE4 0.5 μmol/L. Two- and 6-day experiments were performed and the cell viability was assessed using the MTT assay. All experiments were run in triplicate. The results from cell culture neurotoxicity studies were evaluated by one-way analysis of variance, followed by a Dunnett's test as a post-hoc analysis.

Competitive Inhibition Assay

Inhibition of Aβ1–40 binding to lipidated apoE4 in the presence of Aβ12–28P was analyzed by enzyme-linked immunosorbent assay (ELISA).[38] ApoE4 100 nmol/L was preincubated with an increasing concentration of Aβ12–28P (0 to 400 nmol/L) in 10 mmol/L Tris buffer pH 7.4 for 3 hours at 37°C and then added to immobilized on polystyrene microtiter plates (Immulon-2; Dynatech Lab., Chantilly, VA) Aβ1–40 (10 ng/well).[38] After another 3 hours of incubation, at the same temperature, the plate was washed and apoE4 bound to Aβ1–42 was detected using 3D12 monoclonal antibody (mAb) 1:1000 (Biodesign Int., Saco, MA) followed by incubation with anti-mouse IgG HRP-conjugate (Amersham, Piscataway, NJ) at 1:5000. The color reaction was developed with a 3,3,5,5-tetramethybenzidine substrate (BioRad), and optical density (OD) was measured on a 7520 Microplate Reader (Cambridge Technology, Watertown, MA). Nonspecific binding was determined using bovine serum albumin and/or omitting the apoE4 in the assay. OD values were converted to percentages with the binding of apoE4 in the absence of inhibitor being considered as 100%. The mean ± SD (SD) from three independent duplicate experiments was plotted in Figure 3 and analyzed by a one-site competition non-linear regression fit algorithm using GraphPad Prism version 4.0 (GraphPad Software, San Diego, CA).

Blood-Brain Permeability Studies

Aβ12–28P was labeled with Na[^{125}I] (Amersham) using a two-step reaction. First, sulfo-succinimidyl-4-hydroxy-benzoate was coupled (Sulfo-SHB, Pierce, Rockford, Il) to side chain amino groups of lysine residues (Aβ posi-

tions 16 and 28)[39,40] and then these sites were labeled with Na[^{125}I] using IODO-BEADS (Pierce) according to the manufacturer's instructions. Unbound ^{125}I was removed using a gel filtration column (Bio-Gel P-6, Bio-Rad, Hercules, CA).[41] Aβ1–40, used for comparison, was tagged with Na[^{125}I] using IODO-BEADS directly.

The blood-brain permeability of Aβ12–28P was assessed using the perfusion and capillary depletion techniques[42,43] in 10 C57BLJ wild-type mice (22 to 25 g body weight). Animals were anesthetized by intraperitoneal injection of ketamine HCl (0.12 mg/g) and xylazine (0.016 mg/g)[44] and their neck vessels were dissected as described elsewhere.[42,43] ^{125}I-Aβ12–28P (12.3 nmol) or [125]I -Aβ1–40 (11.6 nmol) and inulin [C[14]]-carboxylic acid (1.33 μCi/mg) as a cerebrovascular space marker (molecular weight = 5175 Da)[45] were injected into the right carotid artery and blood samples were collected from the jugular vein on the ipsilateral side. After the infusion was completed, the brain vasculature was washed out with 20 ml of medium without radiolabeled tracers and the animals were sacrificed by decapitation. The brain was instantly removed from the skull, arachnoid membranes were peeled away, and the choroid plexuses were separated by dissection. The ipsilateral hemisphere was homogenized in phosphate-buffered saline (PBS) (1:10 w/v) with a cocktail of protease inhibitors (Complete, Boehringer Mannheim, Mannheim, Germany) and separated from remaining microvasculature by filtrating the homogenate through mesh nylon net with 60-μm pores.[46] The ^{125}I and ^{14}C radioactivity in the brain and vessel fractions were determined in a Beckman 4000 gamma counter and a Beckman LS-7000 liquid scintillation spectrometer, respectively (Beckman-Coulter, Fullerton, CA).

Brain uptake of radiolabeled Aβ12–28P and Aβ1–40 was expressed as perfusion ratio[47] $V_D = C_{BR}/C_{PL}$, where C_{BR} and C_{PL} are cpm/g of brain and cpm/μl of serum, respectively. The volume of distribution for a given peptide was corrected for capillary uptake by subtracting V_D of inulin from V_D of peptide. V_D of inulin was on average 14 ± 5 μl/g.

Determination of the Half-Life of Aβ12–28P

The half-life of Aβ12–28P was determined after a single bolus injection of 80 μg end-protected ^{125}I-Aβ12–28P into the femoral vein of six anesthetized wild-type C57BL6J mice. Blood samples were collected at several time points and the concentration of radiolabeled peptide in the serum was assessed using the trichloroacetic (TCA) acid precipitation method, as described elsewhere.[45] Bioavailability of ^{125}I-Aβ12–28P following intravenous administration was compared with bioavailability following single intranasal administration of the same dose of peptide (80 μg). This experiment was performed in another six wild-type C57BL6J mice which received a diluted peptide in 10-μl drops instilled into both nostrils over 5 minutes.

Radioactivity measurements at separated time points were transformed into percentage values compared to serum radioactivity following intravenous injections at t =

0 as 100%. The mean ± SD from all tested animals was plotted in Figure 4 and analyzed by a one-phase exponential decay non-linear regression fit algorithm using GraphPad Prism version 4.0. To compare the extent of drug bioavailability after the administration of a single intravenous or intranasal dose the area under both curves were calculated.[48]

Testing Activity of Aβ12–28P in Vivo

Initial testing of Aβ12–28P toxicity *in vivo* was performed on five wild-type C57BL6J mice which received intraperitoneal (i.p.) injections of 1 mg of Aβ12–28P diluted in 0.5 ml of sterile PBS three times per week for 4 weeks. Mice were observed for an additional 2 weeks and all remained alive and well. They were monitored for change in body weight, physical appearance, measurable clinical signs, unprovoked behavior, and response to external stimuli.[49,50] Following sacrifice, sections from the brain, liver, gut, spleen, kidney, and heart were examined using hematoxylin and eosin staining.

The effect of Aβ12–28P on Aβ deposition was tested in APP$^{K670N/M671L}$/PS1^{M146L} double Tg mice.[51–53] There were six Aβ12–28P-treated and six vehicle-treated sex-matched APP$^{K670N/M671L}$/PS1^{M146L} mice in this study. The first administration of Aβ12–28P or vehicle was begun at 4 months of age, at which time the APP$^{K670N/M671L}$/PS1^{M146L} mice already have modest numbers of Aβ lesions.[54,55] The treatment was continued for 4 weeks (1 mg i.p. three times per week) and animals were sacrificed a week after the last injection with an overdose of sodium pentobarbital (150 mg/kg i.p.) and transcardially perfused with PBS and paraformaldehyde as described before.[24,56] The brain was cut into serial, 40-μm thick coronal sections using a freezing microtome (Leica SM2400, Nussloch, Germany). Sections were collected in 10 separated series. Each of them contained a complete set of sections spaced 400-μm apart along the rostro-caudal axis of the brain. Cut sections were stored in cryoprotectant (30% sucrose/30% ethylene glycol in 0.1 mol/L phosphate buffer) at −30°C until stained. Aβ deposits were stained either with 6E10 mAb (raised against residues 1–16 of Aβ[57]) or Thioflavin-S for fibrillar amyloid.[58] Details of used immunohistochemical techniques were published previously.[24,56,58] Sections stained with 6E10 mAb were developed using 3,3-diaminobenzidine tetrahydrochloride with nickel ammonium sulfate and were not counterstained. This produced black staining of Aβ deposits against a transparent background that facilitated selecting density threshold and quantification of Aβ deposits. All brains were stained at one time to avoid variability in the intensity of staining that may occur between different batches.

Aβ deposits were quantified in the neocortex and in the hippocampus using a random, unbiased sampling scheme and semi-automated image analysis system. First, one of the collected series of brain sections were selected for immunostaining with 6E10 mAb using a random number generator. There are on the average 14 to 15 cross-sections throughout the neocortex and seven cross-sections throughout the hippocampus in each series. This gives a similar number of entries for both structures. In the second step the whole profile of the neocortex and the hippocampus as appearing on the coronal plane cross-sections were traced using the Bioquant image analysis system (R&M Biometrics Inc., Nashville, TN), which randomly superimposed a grid (800 μm × 800 μm) over the traced contour. Test areas (640 μm × 480 μm) were applied by the image analysis system over knots of the grid. With such designed sampling schemes, Aβ load was analyzed in 98 ± 16 (mean ± SD) test areas in the neocortex per brain and 31 ± 6 test areas in the hippocampus. About 48% of cross-section area of a structure of interest was covered by a sum of test areas. Efficiency of sampling scheme was verified using an algorithm proposed by West and Gundersen,[59–61] whereby the square of variation coefficient for an experimental group should be more than two times larger than the square of error coefficient calculated for Aβ load in both the neocortex or the hippocampus in an individual animal in this group. If this condition is met, adding more test areas does not enhance the accuracy of stereological measurements.[59] Such a sampling scheme designed in a fully random and unbiased manner helps to counterbalance the natural tendency of Aβ to be deposited in a non-homogenous manner in AD Tg mice.

Images of the test areas were captured and a threshold optical density for immunostained Aβ plaques was obtained. The black color of Aβ deposits and the lack of counterstaining allowed for easy and reliable discrimination of stained objects from the background. Plaques were automatically outlined by the particle analysis protocol of the software, numbered and measured. Objects smaller than 170 μm^2 (average cross-sectional area of a hippocampal pyramidal neuron + 2 standard deviations)[62,63] were filtered out. The sum of all areas of plaques outlined in a test field and their number in a test field was measured. If needed, artifacts such as non-specific meningeal or vascular staining were eliminated manually. Two parameters Aβ load (ie, percentage of test area occupied by Aβ) and numerical density of Aβ plaques (number of plaques in a test area divided by its area − 0.307 mm^2) were calculated. Differences between groups were analyzed by means of the Mann-Whitney *U*-test.

To demonstrate that the observed treatment effect is not associated with an immune response, plasma of animals treated with Aβ12–28P were tested for the presence of antibodies against Aβ using a sandwich ELISA.[24,64] Plasma of animals vaccinated with Aβ homologues peptide, K6Aβ1–30, given with Freund's as an adjuvant, which is known to induce an immune response against Aβ, were used as a positive control.[24] Mouse sera in increasing range of dilution 1:50 to 1:25600 were applied to Immunolon-2, 96-well microtiter plates coated with Aβ1–42 or Aβ1–40 and incubated overnight at 4°C. The plates were then washed in PBS, followed by incubation with goat anti-mouse Ig HRP-conjugate (Amersham). Development of color reaction and OD measurements were performed as described above.

Table 1.   Circular Dichroism Measurements

Time (h)	Aβ1–42			Aβ12–28			Aβ12–28P		
	α-helix	β-sheet	Random coil	α-helix	β-sheet	Random coil	α-helix	β-sheet	Random coil
0	4	49	47	41	2	57	39	2	59
24	2	51	47	41	2	57	39	2	59
96	2	58	40	41	2	57	39	2	59

Measurements of circular dichroism (CD) at different time points shown as a percentage of ∝-helix, β-sheet, and random coil. Peptides were incubated at concentration 100 μmol/L in 5 mmol/L of Tris buffer at 37°C. Values were calculated based on the Lincomb and neural network algorithms.

Results

Studies of Aβ12–28P in Vitro

The secondary structure of peptides was analyzed because an increased β-sheet content of Aβ peptides is a prerequisite for fibril formation and is associated with toxicity. CD measurements performed immediately after reconstitution of peptides with 5 mmol/L Tris buffer (pH 7.0) showed that the secondary structure of Aβ12–28 and Aβ12–28P is dominated by α-helix and random coil, which constitute 41% and 57%, or 39% and 59% of the total protein structure, respectively (Table 1). The β-sheet content of both peptides was minimal (2%), in contrast to Aβ1–42, which had a CD spectrum at time = 0 consistent with 49% β-sheet content. The secondary structure of Aβ12–28 and Aβ12–28P remained stable during the 72 hours of incubation at 37°C, whereas the β-sheet content of Aβ1–42 increased from 49% to 58%. These findings were consistent with analysis of fibrillogenic potentials of the studied peptides using the Thioflavin-T assay. Aβ12–28P did not form any fibrils during 10 days of incubation (Figure 1A). In Aβ12–28 a small amount of fibrils could be detected following 24 hours of incubation which continued to increase until day 6 when fluorescence levels reached a plateau. However, compared to Aβ1–40 or Aβ1–42, the amount of fluorescence emitted by the Aβ12–28 solution was significantly lower ($P < 0.0001$, repeated measures analysis of variance; Aβ12–28 *versus* Aβ1–40 and Aβ12–28 *versus* Aβ1–42 $P < 0.001$, Tukey HSD post-hoc test). This indicated that the fibrillogenic potential of Aβ12–28 is significantly lower than that of full-length Aβ peptides.

Apo E3 and apo E4 act as pathological chaperones in Aβ fibrillization.[3–5,65] In their presence, the amount of fibrils formed by Aβ1–42 over time was significantly increased (Figure 1B). However, when apo E3 or apo E4 were preincubated with Aβ12–28P before addition to the Aβ1–42 solution, a significantly lower amount of fluorescence was recorded over time ($P < 0.0001$, repeated measures analysis of variance; $P < 0.01$ and $P < 0.05$ Tukey HSD post-hoc test for specific effect of Aβ12–28P on Apo E4 and apo E3, respectively). After a 24-hour incubation, a relative reduction in fluorescence by 25.3% was observed for apo E4 and by 14.5% for apo E3, whereas by day 6 the reductions were 50.9% and 54.1% respectively. There were no significant differences between curves produced by Aβ1–42 in the presence of apo E3 and E4 inhibited by Aβ12–28P and Aβ1–42 alone

or Aβ1–42 with Aβ12–28P. However, within 24 hours of incubation the fluorescence of Aβ1–42 with apo E and Aβ12–28P were higher than those produced by Aβ1–42 alone or Aβ1–42 with Aβ12–28P. Differences between Aβ1–42 incubated in the presence of apo E4 and apo E3
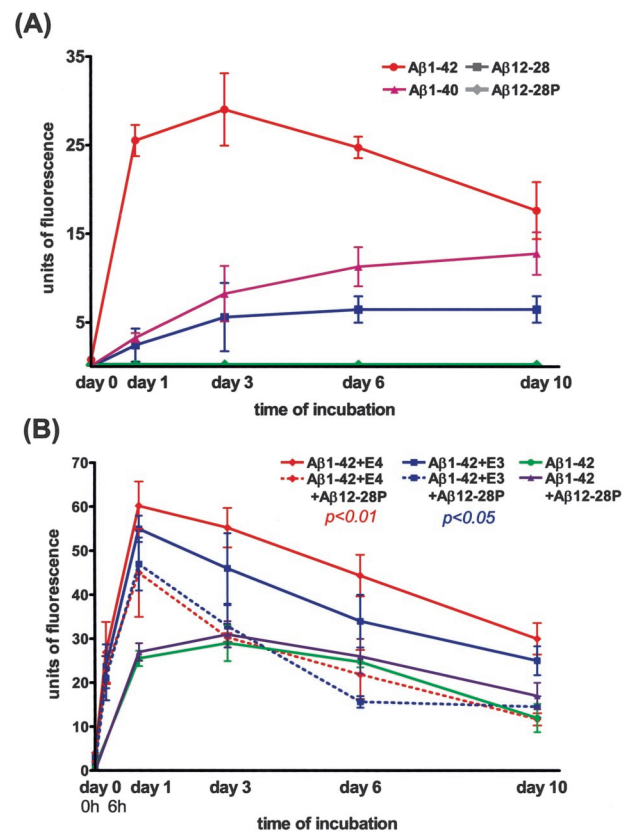
Figure 1. A: Thioflavin-T assay demonstrates the modest ability of Aβ12–28 to form fibrils which is significantly lower than Aβ1–40 and Aβ1–42 ($P < 0.0001$, repeated measures analysis of variance; $P < 0.001$ Aβ12–28 *versus* Aβ1–40 and Aβ12–28 *versus* Aβ1–42 Tukey HSD post-hoc test). No fibrils were formed by Aβ12–28P. **B:** Aβ1–42 was incubated in the presence of either apo E3 or apo E4 (**solid red** and **blue lines**) that significantly increased amount of fibrils formed over time compared with Aβ1–42 alone (**green line**; $P < 0.0001$, repeated measures analysis of variance; $P < 0.01$ and $P < 0.05$ Tukey HSD post-hoc test for specific comparison of Aβ1–42+apo E4 and Aβ1–42+apo E3 *versus* Aβ1–42 alone, respectively). Chaperoning effect of apo E4 and apo E3 on Aβ1–42 fibril formation was significantly reduced if apo E was preincubated with equimolar concentrations of Aβ12–28P (**dashed red** and **blue lines**; $P < 0.01$ and $P < 0.05$ Tukey HSD post-hoc test for specific effect of Aβ12–28P on Apo E4 and apo E3, respectively). There were no significant differences between fibrillization curves of Aβ1–42 incubated with apo E4 and Aβ12–28P or apo E3 and Aβ12–28P *versus* Aβ1–42 incubated alone. Aβ12–28P alone had no significant effect on Aβ1–42 fibril formation.

(A)

(B)
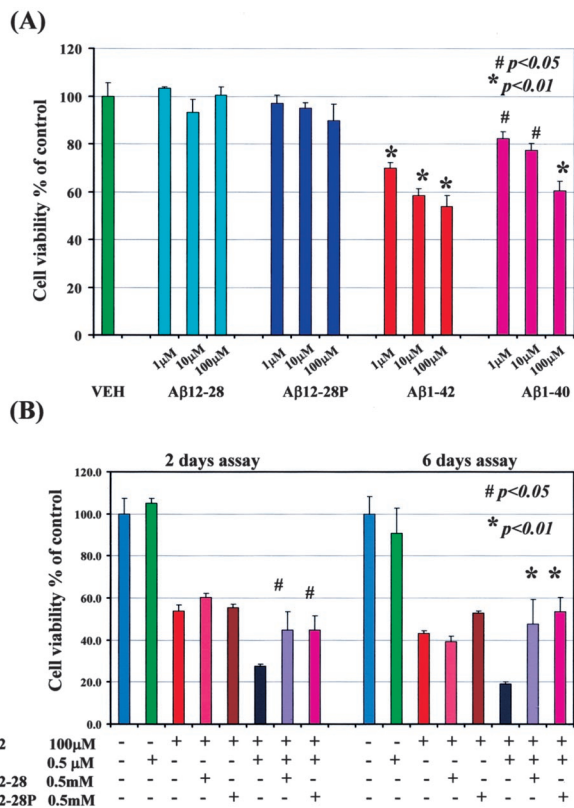
Figure 2. Cytotoxicity assay using SK-N-SH human neuroblastoma cells. **A:** No significant reduction in viability was observed when cells were incubated with Aβ12–28 or Aβ12–28P. In contrast, even the lowest concentration of Aβ1–40 or Aβ1–42 resulted in significant cytotoxic effect (one-way analysis of variance $P < 0.0001$, post-hoc Dunnett's test $P < 0.01$ for Aβ1–42 and $P < 0.05$ for Aβ1–40 *versus* control) VEH-vehicle. **B:** Toxicity of Aβ1–42 in cell culture was potentiated in the presence of apo E4 ($P < 0.01$ Aβ1–42 *versus* Aβ1–42/apo E4). This chaperoning effect of apo E could be neutralized if apo E4 was preincubated with Aβ12–28 or Aβ12–28P (Aβ1–42/apo E4 *versus* Aβ1–42/apo E4/Aβ12–28 or Aβ1–42/apo E4/Aβ12–28P $P < 0.05$ for 2-day assay and $P < 0.01$ for 6-day assay). Apo E alone did not reduce cell viability. Slightly increased cell viability was observed if Aβ1–42 was incubated with Aβ12–28P without apo E for 6 days ($P < 0.05$), but not for 2 days. Adding Aβ12–28 to Aβ1–42 did not alter cell viability. For clarity of the figure, only significance between Aβ1–42/apo E4 *versus* Aβ1–42/apo E4/Aβ12–28 and Aβ1–42/apo E4/Aβ12–28P were marked.

versus Aβ1–42 alone or Aβ1–42 with Aβ12–28P were statistically significant ($P < 0.01$; and $P < 0.05$). This indicates that in a presence of Aβ12–28P both apo E3 and apo E4 have a reduced ability to promote the fibril formation of Aβ1–42. Aβ12–28P alone had no significant effect on Aβ1–42 fibrillogenesis.

No significant reduction in the viability of SK-N-SH human neuroblastoma cells was observed when cells were incubated with Aβ12–28 or Aβ12–28P at a concentration ranging from 1 μmol/L to 100 μmol/L (Figure 2A). In contrast, a significantly reduced viability of SK-N-SH cells was noted after a 2-day incubation with Aβ1–40 or Aβ1–42 starting from concentration as low as 1 μmol/L ($P < 0.05$ for Aβ1–40 and $P < 0.01$ for Aβ 1–42).

In a separate experiment, Aβ1–42 (100 μmol/L) was incubated with apo E4 (0.5μmol/L). This produced a significantly greater reduction in cell viability compared to incubation with Aβ1–42 alone ($P < 0.01$ [Figure 2B]). If the apo E4 was preincubated with an equimolar concentration of either Aβ12–28 or Aβ12–28P before adding
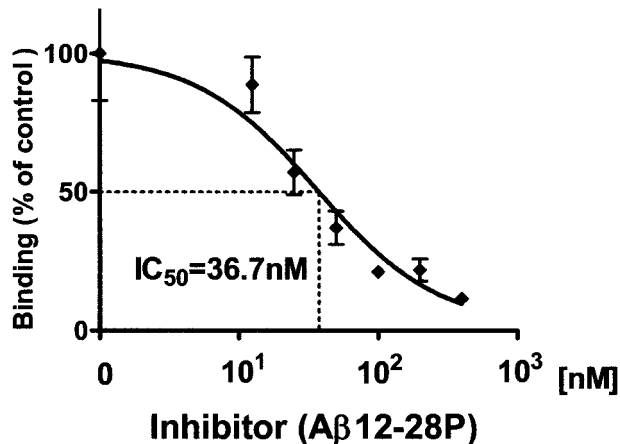

Figure 3. In a competitive inhibition assay, Aβ12–28P (0 to 400 nmol/L/L) was preincubated with 100 nmol/L apoE4 and added to Aβ1–40 coated wells. Results are expressed as a percentage of residual apo E4 binding, considering binding of apoE4 in the absence of inhibitor as 100%. Data representing the mean ± SD of three independent duplicate experiments were fitted into one-site competition curve. Half of maximal inhibition (IC_{50}) was calculated to be 36.7 nmol/L.

to Aβ1–42 a significant rescue of the cell viability could be demonstrated ($P < 0.05$ for the 2-day time point and $P < 0.01$ for the 6-day time point). The viability of SK-N-SH cells incubated in the presence of apo E4 alone (0.5 μmol/L) was not significantly reduced compared to the control group (only vehicle added). Slightly increased cell viability was observed if Aβ1–42 (100 μmol/L) was incubated with Aβ12–28P (0.5 μmol/L) without apo E for 6 days ($P < 0.05$), but not for 2 days.

Pharmacokinetic and Blood-Brain Barrier Permeability Studies

A competitive inhibition assay was performed to demonstrate the ability of Aβ12–28P to specifically bind to apoE and block the binding to the full-length Aβ peptide. Preincubation of apoE4 with increasing concentrations of Aβ12–28P resulted in decreased affinity toward immobilized Aβ1–40 (Figure 3). The concentration of Aβ12–28P producing half-maximal inhibition (IC_{50}) was calculated from a non-linear regression, one-site competition curve as 36.7 nmol/L. The inhibition constant (K_I) of Aβ12–28P was calculated to be 11.37 nmol, given the known dissociation constant (K_D) of Aβ1–40 binding to apoE is approximately 10 nmol.[14,66]

Aβ12–28P was synthesized from D-amino acids and end-protected to prevent its biodegradation and extend its potential therapeutic effect. The plasma half-life of Aβ12–28P was estimated from intravenous injection of a single dose of ^{125}I-Aβ12–28P experiment to be 62.2 ± 18 minutes (mean ± SD) (Figure 4). This contrasts with a plasma half life of 2 to 3 minutes for non-end-protected Aβ1–40.[67] The presence of [125]I- Aβ12–28P in the serum could also be demonstrated following intranasal administration. At t = 0 the serum level was equal to about 40% of the level achieved after administration of the same amount of peptide intravenously. In contrast to the serum profile, where the level of peptide decreased sharply,
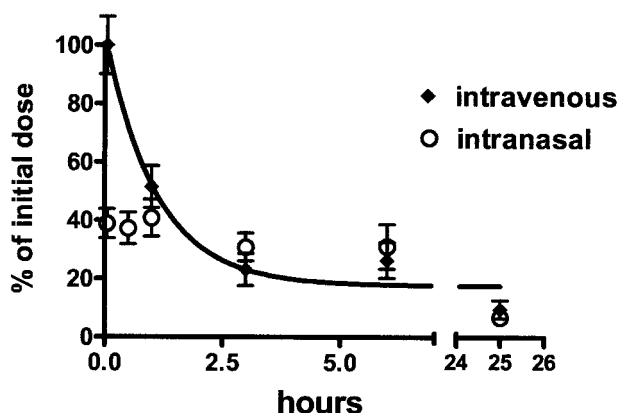
Figure 4. Serum level of ^{125}I-Aβ12–28P following single intravenous (**dia-monds**) or intranasal (**open circles**) dose. Values represent percentage of drug serum level considering drug serum level at t = 0 after intravenous administration as 100%. Values are expressed as mean ± SD for all animals studied (*n* = 6 for intravenous and *n* = 5 for intranasal). The half-life of Aβ12–28P following single intravenous injection was analyzed using one-phase exponential decay non-linear regression fit algorithm. It was calculated to be 62.2 ± 18 minutes.

following intranasal administration, the serum level remained stable for the first hour and then started to decrease slowly, matching the level of peptide after intravenous administration at t = 3 hours. However, when the areas under the curve for intravenous and intranasal administration were calculated, no significant differences were found. This indicates that the extent of drug bioavailability after intravenous administration is comparable to bioavailability of the same dose administered intranasally.

An inhibitor of apoE/Aβ binding has to be able to cross the BBB to exert its therapeutic effect. The BBB permeability of Aβ12–28P was studied using the brain perfusion and capillary depletion techniques. The volume of distribution (V_D) of [125]I- Aβ12–28P after *trans*-carotid perfusion was calculated to be 65 ± 20 μl/gram of brain tissue (mean ± SD) whereas the V_D of [125]I- Aβ1–40 under the same experimental conditions was 81.3 ± 40 μl/gram (difference not statistically significant). More than 90% of [125]I- Aβ12–28P was found in the capillary-depleted brain fraction indicating that the majority of the peptide crossed into the brain parenchyma and was not retained in the vascular compartment.

Reduction of Aβ-Load in APP/PS1 Mice after Aβ12–28P Treatment

Before testing the effect of Aβ12–28P on Aβ load in Tg mice, a toxicity test was carried out using five wild-type mice which received 1 mg of Aβ12–28P three times a week for 4 weeks; the same protocol later used on the Tg mice. No changes were noted in treated animals in terms of body weight, physical appearance, unprovoked behavior or response to external stimuli. Hematoxylin and eosin-stained sections of the brain, heart, liver, gut, spleen, or kidneys did not reveal any pathology.

Treatment with Aβ12–28P was started at the age of 4 months. After 4 weeks of peptide administration, the Aβ load in the neocortex and in the hippocampus of treated
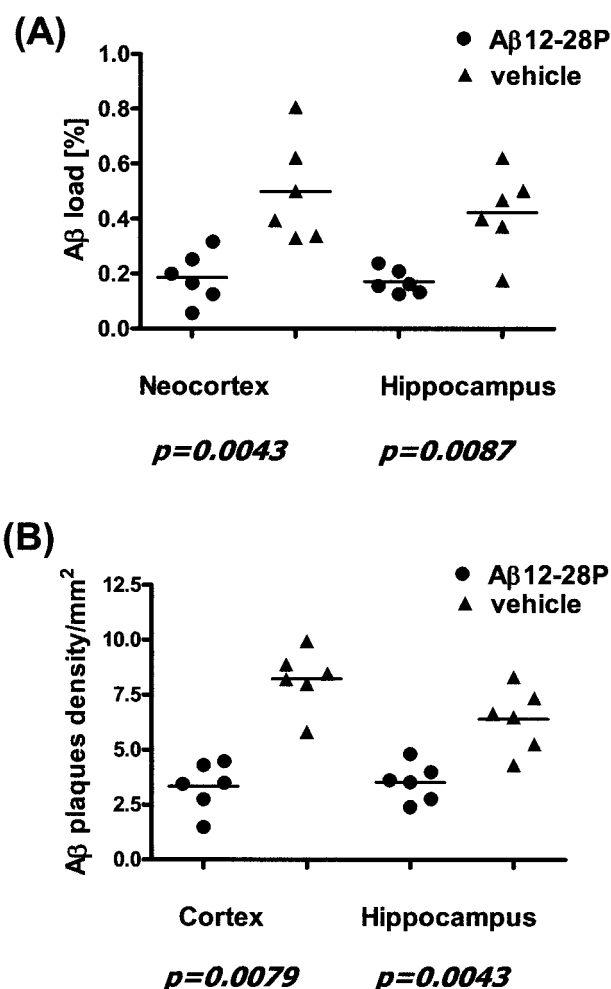
Figure 5. Significant reduction in the area covered by Aβ (Aβ load [A]) and in numerical density of Aβ plaques [B] was observed in APP [K670N/M671L/] PS1[M146L] Tg mice treated with Aβ12–28P compared to age-matched Tg control animals treated with placebo.

animals was 63.3% (*P* = 0.0043) and 59.5% (*P* = 0.0087) lower compared to age-matched control Tg animals, which received vehicle (Figure 5A and Figure 6, A and B). There was also a reduction in the numerical density of Aβ plaques in treated mice by 60.1% in the neocortex (*P* = 0.0079) and by 49.6% in the hippocampus (*P* = 0.0043) (Figure 5B). The reduction in the density of Aβ plaques was also seen on Thioflavin-S staining which selectively labels Aβ deposits in a fibrillar form (Figure 7).

Treatment with Aβ12–28P had a marked effect on reducing the density of plaques in all size categories. There was a 52.8% reduction in the density of small plaques (cross-section area < 500 μm², *P* < 0.0043), a 53.5% reduction in the number of medium-size plaques (cross-section area > 500 μm² and < 1000 μm²; *P* < 0.05), and a 44% reduction in the number of large plaques (> 1000 μm²; non-significant) in the neocortex (Figure 8A). In the hippocampus, the reduction in the density of plaques in each size category was 37.6% for small plaques (*P* < 0.05), 48.6% for medium-size plaques (*P* < 0.05), and 65.4% for large plaques (*P* < 0.05, Figure 8B).
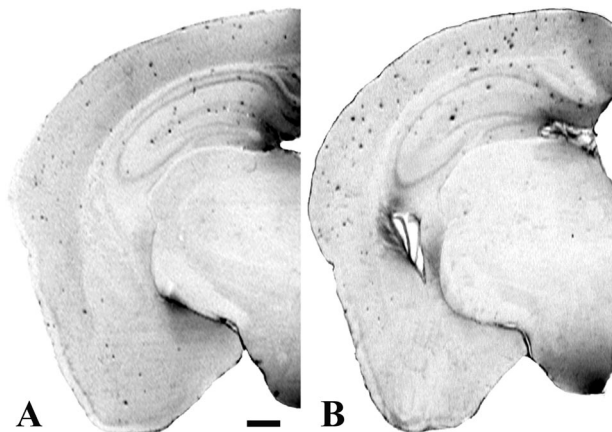
Figure 6. Hemispheric sections of APP$^{K670N/M671L}$/PS1^{M146L} Tg mice treated with Aβ12–28P (**A**) and with vehicle (**B**). Reduced density of Aβ deposits following 4 weeks of treatment with Aβ12–28P is evident compared to age-matched control double Tg. 6E10 mAb immunohistochemistry; **bar**, 500μm.

At the time of sacrifice, sera of wild-type and Tg mice treated with Aβ12–28P were collected and tested for presence of anti-Aβ antibodies. No anti-Aβ antibodies were detected in mice treated with Aβ12–28P, whereas under the same conditions, positive control, sera of APP$^{K670N/M671L}$ mice immunized with K6Aβ1–30-NH$_2$ and Freund's adjuvant,[24] showed the presence of anti-Aβ antibodies with a titer ranging from 1:1000 to 1:10,000. This indicates that the effect of Aβ12–28P on Aβ load cannot be attributed to a humoral response against Aβ.

Discussion

Accumulation of Aβ, a 39–43 amino acid peptide, in brains of AD patients is a hallmark of AD pathology.[68] Complementary pieces of evidences derived from *in vivo* and *in vitro* studies have demonstrated that apoE critically promotes Aβ fibrillization and deposition.[20] The most striking example, emphasizing the role of apoE as a pathological chaperone of β -amyloidosis comes from
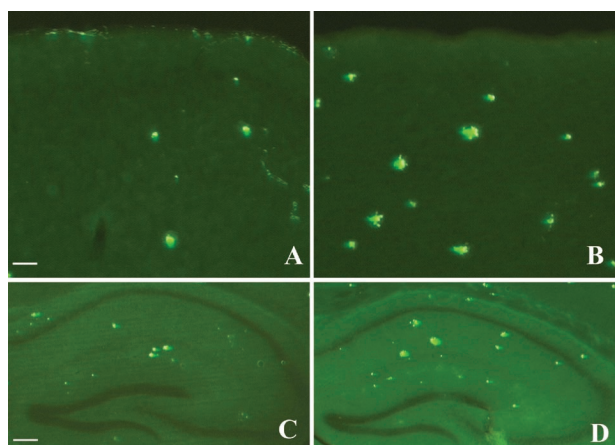
Figure 7. Reduction in numerical density and cross-section area of plaques were also noticed on sections stained with Thioflavin-S for fibrillar Aβ. **A** and **C**, treated animals; **B** and **D**, vehicle. **A** and **B**, neocortex; **bar**, 500 μm. **C** and **D**, hippocampus; **bar**, 125 μm.

(A) NEOCORTEX
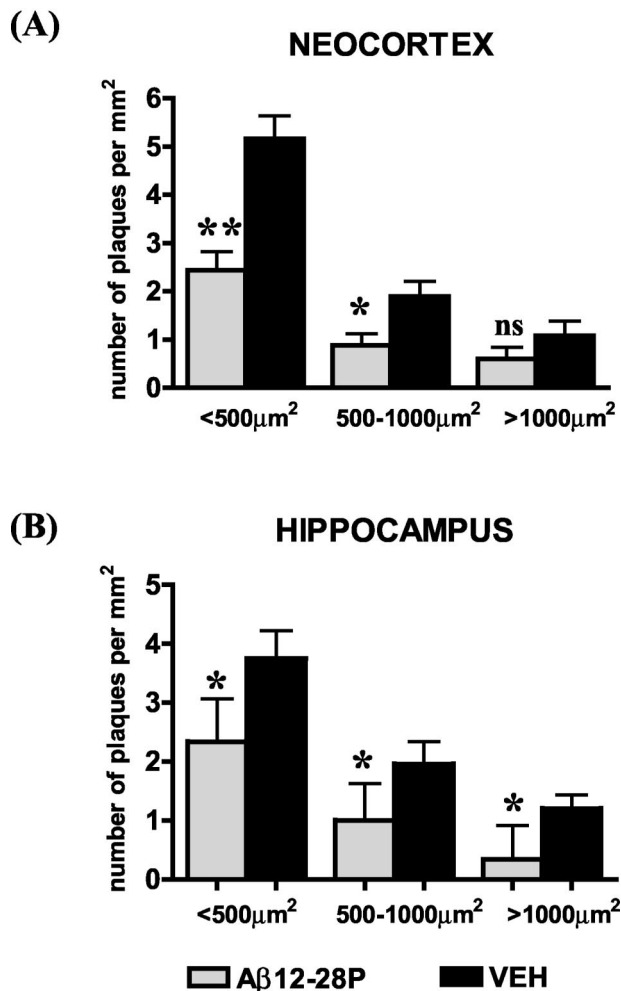
(B) HIPPOCAMPUS

Figure 8. Treatment with Aβ12–28P resulted in reduced number of small (< 500 μm^2), medium-sized (> 500-< 1000 μm^2), and large plaques (> 1000 μm^2) both in the cortex (**A**) and in the hippocampus (**B**). This demonstrates an effect of inhibition of pathological chaperones on the development of new Aβ plaques. *, $P < 0.05$; **, $P < 0.01$, Mann-Whitney *U*-test.

experiments with generation of APP^{V717F}/apoE$^{-/-}$ mice which have a delayed onset of Aβ deposition, a reduced Aβ load, and no fibrillar Aβ deposits, compared to APP^{V717F}/apoE$^{+/+}$ Tg mice. APP^{V717F}/apoE$^{+/-}$ mice demonstrate an intermediate level of pathology.[12,69–71] Neutralization of the chaperoning effect of apoE would therefore have a mitigating effect on Aβ accumulation. To investigate this potentially therapeutic mechanism, we synthesized a peptide homologous to residues 12–28 of Aβ which is a specific apoE binding domain.[13,18] Such peptide could attach to apoE preventing its binding to the full-length Aβ.[20] To avoid intrinsic toxicity associated with its residual capacity to form fibrils and hence ability to co-deposit on existing plaques, the sequence of Aβ12–28 was modified by replacing valine for proline in position 18. This rendered Aβ12–28P non-fibrillogenic, as demonstrated by CD and Thioflavin-T aggregation assays, as well as non-toxic in cell culture. These modifications did not modify the affinity of Aβ12–28P to apoE. In a competitive inhibition assay, Aβ12–28P reacted with lipidated apoE preventing its binding to full-length Aβ

with $IC_{50} = 36.7$ nmol/L. An effect of apoE on Aβ fibril formation and toxicity in cell culture was significantly reduced in the presence of Aβ12–28P. Synthesis of Aβ12–28P with end-protection and using of D-amino acids extended its half-life in the serum to 62 minutes, contrasting with the very short half-life of L-amino acid, non-end-protected Aβ1–40 (2 to 3 minutes).[67] Aβ12–28P is BBB permeable allowing for an *in vivo* effect within the brain. APP[K670N/M671L]/PS1[M146L] AD Tg mice treated with Aβ12–28P had a significantly lower Aβ load, similar to what is observed in mice with decreased apoE expression.[12,69–71] The initial Aβ plaques in APP[K670N/M671L]/PS1[M146L] mice appear at 3 months of age; whereas, between the fourth and the fifth months of life, Aβ deposition follows an exponential curve where new plaques are actively formed.[54] We show that administration of Aβ12–28P for a period as short as 1 month resulted in an over twofold reduction in Aβ load and plaque density compared to untreated age-matched Tg animals. An effect of Aβ12–28P on Aβ deposition occurs without a humoral response since we did not detect any anti-Aβ antibodies in the sera of treated animals.

Little is known about dynamic plaque growth *in vivo*. Early, *in vitro* models have suggested that Aβ deposits may grow by deposition of soluble Aβ[72] and that apo E is critical for this process (for review, see Tomiyama et al[3]). More recently, Christie et al[73] using *in vivo* multiphoton microscopy demonstrated that the size of already formed Aβ deposits remains unchanged in 18-month-old Tg2776 AD Tg mice over 5 months of longitudinal observations. In addition, an average diameter of a plaque stained with Thioflavin-S in Tg mouse brain does not change appreciably between 12 and 22 months, although plaque density increases between these time points almost sixfold.[73] In our study, treated mice showed a decreased density of plaques in all size categories implying that blocking the Aβ/apo E interaction *in vivo* decreases the rate of new plaque formation. Whether or not this form of treatment may also have an effect on the growth dynamic of plaques remains to be confirmed.

Although *in vitro* Aβ homologous peptides can aggregate and form fibrils spontaneously, with apo E acting only to accelerate this process,[4,5] it is likely that *in vivo* Aβ oligomerization and deposition is much more dependent on the presence of apo E.[74] *In vitro* fibrillization experiments demonstrated that proportionally minute amount of apoE can exert a chaperoning effect with molar Aβ:apoE ratio being 100 to 200:1.[4,5] This shows that a very small amount of apoE is sufficient to propagate fibril formation and indicates that only a small amount of apoE has to be pharmacologically targeted. Therefore even with limited BBB permeability, a therapeutic effect of Aβ12–28P could be demonstrated *in vivo*.

The pharmacological targeting of apoE has to take into account that apoE is involved in the clearance of Aβ from the central nervous system (CNS) across the BBB in addition to a role as a pathological chaperone.[75,76] ApoE KO mice and mice expressing human apoE4 on murine apoE KO background have impaired clearance of synthetic Aβ injected into the brain parenchyma compared to mice expressing human isoform apoE3.[77] Therefore,

apoE plays a dual role in Aβ clearance and deposition, which is likely dependent on the concentration of CNS Aβ and that of other Aβ binding proteins. Given the opposing roles apoE has on Aβ peptides in the CNS, it is conceivable that blocking apoE/Aβ binding would increase the amyloid burden. However, it appears that the role of apo E as a pathological chaperone outweighs its role in Aβ clearance since APP[V717F]/apoE^{−/−} mice have a decrease in both Aβ load and level.[12,69–71] Similarly, our pharmacological blocking of the Aβ/apoE interaction in this study is consistent with the dominance of a pathological chaperone function. Evidence comparing Aβ levels in APP[V717F] Tg mouse strains crossed to either apoE or apoJ KO lines suggest that apoJ and apoE can effectively replace each other in their Aβ clearance function. It is only when both apoJ and apoE are knocked out that Aβ amyloid deposition is increased.[78]

AD is a progressive disease for which only palliative treatment is currently available. A number of potential new therapeutic approaches targeting pathological biology of AD, and β-amyloidosis in particular, are emerging. The vaccination approach has shown great promise in model animals;[24,79–81] however, human trials have shown toxicity to be a major problem.[82] Targeting the secretase enzymes which are responsible for releasing Aβ from APP has also been a major therapeutic focus. However, these enzymes are involved in several other functions[83–86] and selective inhibition of Aβ cleavage without associated significant toxicity is a substantial issue. Compared to vaccination[87] or γ-secretase inhibitors,[88] blocking of pathological chaperones is not associated with the risk of an autoimmune reaction or affecting multiple signaling pathways including Notch-1 and wnt.[86] Animals treated with Aβ12–28P did not produce a humoral response related to the peptide's small size and because no adjuvant was administered. Our data demonstrates that inhibiting Aβ/apoE interaction over a relatively short period of time can have dramatic effects on amyloid burden, highlighting the importance of apoE in the balance of clearance *versus* aggregation/deposition of Aβ. Therefore, inhibitors of Aβ pathological chaperones may be an alternative approach for the treatment of AD amyloidosis. Results of this initial study make this concept worthy of further exploration including biochemical and behavioral characterization of treatment effects in various AD Tg models co-expressing familial AD-linked mutations and the different allelic forms of the human apoE gene.

References

1. Selkoe DJ: The origins of Alzheimer disease: a is for amyloid. JAMA 2000, 283:1615–1617
2. Barrow CJ, Yasuda A, Kenny PT, Zagorski MG: Solution conformations and aggregational properties of synthetic amyloid β-peptides of Alzheimer's disease: analysis of circular dichroism spectra. J Mol Biol 1992, 225:1075–1093
3. Tomiyama T, Corder EH, Mori H: Molecular pathogenesis of apolipoprotein E-mediated amyloidosis in late-onset Alzheimer's disease. Cell Mol Life Sci 1999, 56:268–279
4. Wisniewski T, Castaño EM, Golabek AA, Vogel T, Frangione B: Ac-

celeration of Alzheimer's fibril formation by apolipoprotein E in vitro. Am J Pathol 1994, 145:1030–1035

5. Ma J, Yee A, Brewer Jr HB, Das S, Potter H: Amyloid-associated proteins α 1-antichymotrypsin and apolipoprotein E promote assembly of Alzheimer β-protein into filaments. Nature 1994, 372:92–94

6. Johnson LV, Leitner WP, Rivest AJ, Staples MK, Radeke MJ, Anderson DH: The Alzheimer's A β-peptide is deposited at sites of complement activation in pathologic deposits associated with aging and age-related macular degeneration. Proc Natl Acad Sci USA 2002, 99:11830–11835

7. Castaño EM, Prelli F, Wisniewski T, Golabek AA, Kumar RA, Soto C, Frangione B: Fibrillogenesis in Alzheimer's disease of amyloid β peptides and apolipoprotein E. Biochem J 1995, 306:599–604

8. Schmechel DE, Saunders AM, Strittmatter WJ, Crain BJ, Hulette CM, Joo SH, Pericak-Vance MA, Goldgaber D, Roses AD: Increased amyloid β-peptide deposition in cerebral cortex as a consequence of apolipoprotein E genotype in late-onset Alzheimer disease. Proc Natl Acad Sci USA 1993, 90:9649–9653

9. Rebeck GW, Reiter JS, Strickland DK, Hyman BT: Apolipoprotein E in sporadic Alzheimer's disease: allelic variation and receptor interactions. Neuron 1993, 11:575–580

10. Yamaguchi H, Sugihara S, Ogawa A, Oshima N, Ihara Y: Alzheimer β amyloid deposition enhanced by ApoE ϵ 4 gene precedes neurofibrillary pathology in the frontal association cortex of non-demented senior subjects. J Neuropathol Exp Neurol 2001, 60:731–739

11. Golabek AA, Soto C, Vogel T, Wisniewski T: The interaction between apolipoprotein E and Alzheimer's amyloid β-peptide is dependent on β-peptide conformation. J Biol Chem 1996, 271:10602–10606

12. Bales KR, Verina T, Dodel RC, Du YS, Altstiel L, Bender M, Hyslop P, Johnstone EM, Little SP, Cummins DJ, Piccardo P, Ghetti B, Paul SM: Lack of apolipoprotein E dramatically reduces amyloid β-peptide deposition. Nat Genet 1997, 17:263–264

13. Strittmatter WJ, Saunders AM, Schmechel D, Pericak-Vance M, Enghild J, Salvesen GS, Roses AD: Apolipoprotein E: high-avidity binding to β-amyloid and increased frequency of type 4 allele in late-onset familial Alzheimer disease. Proc Natl Acad Sci USA 1993, 90:1977–1981

14. Wisniewski T, Golabek AA, Matsubara E, Ghiso J, Frangione B: Apolipoprotein E: binding to soluble Alzheimer's β-amyloid. Biochem Biophys Res Commun 1993, 192:359–365

15. Naslund J, Thyberg J, Tjernberg LO, Wernstedt C, Karlstrom AR, Bogdanovic N, Gandy SE, Lannfelt L, Terenius L, Nordstedt C: Characterization of stable complexes involving apolipoprotein E and the amyloid β peptide in Alzheimer's disease brain. Neuron 1995, 15: 219–228

16. Golabek AA, Marques M, Lalowski M, Wisniewski T: Amyloid β binding proteins in vitro and in normal human cerebrospinal fluid. Neurosci Lett 1995, 191:79–82

17. Shuvaev VV, Siest G: Interaction between human amphipathic apolipoproteins and amyloid β-peptide: surface plasmon resonance studies. FEBS Lett 1996, 383:9–12

18. Strittmatter WJ, Weisgraber KH, Huang DY, Dong LM, Salvesen GS, Pericak-Vance M, Schmechel D, Saunders AM, Goldgaber D, Roses AD: Binding of human apolipoprotein E to synthetic amyloid β peptide: isoform-specific effects and implications for late-onset Alzheimer disease. Proc Natl Acad Sci USA 1993, 90:8098–8102

19. Petkova AT, Ishii Y, Balbach JJ, Antzutkin ON, Leapman RD, Delaglio F, Tycko R: A structural model for Alzheimer's β-amyloid fibrils based on experimental constraints from solid state NMR. Proc Natl Acad Sci USA 2002, 99:16742–16747

20. Ma J, Brewer BH, Potter H, Brewer Jr HB: Alzheimer Aβ neurotoxicity: promotion by antichymotrypsin, apoE4; inhibition by Aβ-related peptides. Neurobiol Aging 1996, 17:773–780

21. Gorevic PD, Castaño EM, Sarma R, Frangione B: Ten to fourteen residue peptides of Alzheimer's disease protein are sufficient for amyloid fibril formation and its characteristic x-ray diffraction pattern. Biochem Biophys Res Commun 1987, 147:854–862

22. Wengenack TM, Curran GL, Poduslo JF: Targeting Alzheimer amyloid plaques in vivo. Nat Biotech 2000, 18:868–872

23. Sigurdsson EM, Permanne B, Soto C, Wisniewski T, Frangione B: In vivo reversal of amyloid β lesions in rat brain. J Neuropathol Exp Neurol 2000, 59:11–17

24. Sigurdsson EM, Scholtzova H, Mehta P, Frangione B, Wisniewski T: Immunization with a non-toxic/non-fibrillar amyloid-β homologous

peptide reduces Alzheimer's disease associated pathology in transgenic mice. Am J Pathol 2001, 159:439–447

25. Matsubara E, Soto C, Governale S, Frangione B, Ghiso J: Apolipoprotein J and Alzheimer's amyloid β solubility. Biochem J 1996, 316:671–679

26. Stine WB, Dahlgren KN, Krafft GA, LaDu MJ: In vitro characterization of conditions for amyloid-β peptide oligomerization and fibrillogenesis. J Biol Chem 2003, 278:11612–11622

27. Fagan AM, Holtzman DM, Munson G, Mathur T, Schneider D, Chang LK, Getz GS, Reardon CA, Lukens J, Shah JA, LaDu MJ: Unique lipoproteins secreted by primary astrocytes from wild-type, apoE (−/−), and human apoE transgenic mice. J Biol Chem 1999, 274: 30001–30007

28. DeMattos RB, Brendza RP, Heuser JE, Kierson M, Cirrito JR, Fryer J, Sullivan PM, Fagan AM, Han XL, Holtzman DM: Purification and characterization of astrocyte-secreted apolipoprotein E and J-containing lipoproteins from wild-type and human apoE transgenic mice. Neurochem Int 2001, 39:415–425

29. Sun YL, Wu S, Bu GJ, Onifade MK, Patel SN, LaDu MJ, Fagan AM, Holtzman DM: Glial fibrillary acidic protein-apolipoprotein E (apoE) transgenic mice: astrocyte-specific expression and differing biological effects of astrocyte-secreted apoE3 and apoE4 lipoproteins. J Neurosci 1998, 18:3261–3272

30. Soto C, Golabek AA, Wisniewski T, Castaño EM: Alzheimer's soluble β-amyloid is conformationally modified by apolipoproteins in vitro. Neuroreport 1996, 7:721–725

31. Greenfield N, Fasman GD: Computed circular dichroism spectra for the evaluation of protein conformation. Biochemistry 1969, 8:4108–4115

32. Perczel A, Park K, Fasman GD: Analysis of circular dichroism spectrum of proteins using the convex constraint algorithim. Anal Biochem 1992, 203:83–93

33. Manavalan P, Johnson C: Variable selection method improves the prediction of protein secondary structure from circular dichroism. Anal Biochem 1987, 167:76–85

34. Toumadje A, Alcorn SW, Johnson C: Extending CD spectra of proteins to 168nm improves the analysis for secondary structures. Anal Biochem 1992, 200:321–331

35. Sreerma N, Woody RW: A self-consistent method for the analysis of protein secondary structure from circular dichroism. Anal Biochem 1993, 209:32–44

36. Shen Y, Sullivan T, Lee CM, Meri S, Shiosaki K, Lin CW: Induced expression of neuronal membrane attack complex and cell death by Alzheimer's β-amyloid peptide. Brain Res 1998, 796:187–197

37. Wei WL, Wang XT, Kusiak JW: Signaling events in amyloid β-peptide-induced neuronal death and insulin-like growth factor I protection. J Biol Chem 2002, 277:17649–17656

38. Matsubara E, Frangione B, Ghiso J: Characterization of apolipoprotein J-Alzheimer's A β interaction. J Biol Chem 1995, 270:7563–7567

39. Bolton AE, Hunter WM: Labeling of proteins to high-specific radioactivities by conjugation to A I-125-containing acylating agent: application to radioimmunoassay. Biochem J 1973, 133:529–538

40. Vaidyanathan G, Affleck DJ, Zalutsky MR: Radioiodination of proteins using N-succinimidyl 4-hydroxy-3-iodobenzoate. Bioconjug Chem 1993, 4:78–84

41. Haugland RP, Bhalgat MK: Preparation of avidin conjugates. The Protein Protocols Handbook. Edited by Walker JM. Totowa NJ, Humana Press, 2002, pp 365–374

42. Zlokovic BV, Martel CL, Mackic JB, Matsubara E, Wisniewski T, McComb JG, Frangione B, Ghiso J: Brain uptake of circulating apolipoproteins J and E complexed to Alzheimer's amyloid β. Biochem Biophys Res Commun 1994, 205:1431–1437

43. Zlokovic BV, Ghiso J, Mackic JB, McComb JG, Weiss MH, Frangione B: Blood-brain barrier transport of circulating Alzheimer's amyloid β. Biochem Biophys Res Commun 1993, 197:1034–1040

44. Grutzendler J, Kasthuri N, Gan WB: Long-term dendritic spine stability in the adult cortex. Nature 2002, 420:812–816

45. Deane R, Yan SD, Submamaryan RK, Larue B, Jovanovic S, Hogg E, Welch D, Manness L, Lin C, Yu J, Zhu H, Ghiso J, Frangione B, Stern A, Schmidt AM, Armstrong DL, Arnold B, Liliensiek B, Nawroth P, Hofman F, Kindy M, Stern D, Zlokovic B: RAGE mediates amyloid-β peptide transport across the blood-brain barrier and accumulation in brain. Nat Med 2003, 9:907–913

46. Lalowski M, Golabek AA, Lemere CA, Selkoe DJ, Wisniewski HM,

Beavis RC, Frangione B, Wisniewski T: The "non-amyloidogenic" p3 fragment (Aβ17–42) is a major constituent of Down syndrome cerebellar preamyloid. J Biol Chem 1996, 271:33623–33631

47. Permanne B, Adessi C, Saborio GP, Fraga S, Frossard MJ, Van Dorpe J, Dewachter I, Banks WA, Van Leuven F, Soto C: Reduction of amyloid load and cerebral damage in a transgenic mouse model of Alzheimer's disease by treatment with a β-sheet breaker peptide. EMBO J 2002, 16:U165–U188

48. Shargel L, Yu CEA: Applied Biopharmaceutics and Pharmakokinetics. New York, McGraw-Hill, 1999

49. Morton DB, Griffiths PH: Guidelines on the recognition of pain, distress, and discomfort in experimental animals and an hypothesis for assessment. Vet Rec 1985, 116:431–436

50. Stokes A: Humane endpoints in animal experiments for laboratory animals used in toxicity testing. Proceedings of the 3rd World Congress on Alternatives and Animal Use in Life Sciences. Bologna, Italy, 1999

51. Hsiao KK, Chapman P, Nilsen S, Eckman C, Harigaya Y, Younkin S, Yang F, Cole G: Correlative memory deficits, Aβ elevation and amyloid plaques in transgenic mice. Science 1996, 274:99–102

52. Duff K, Eckman C, Zehr C, Yu X, Prada CM, Perez-Tur J, Hutton M, Buee L, Harigaya Y, Yager D, Morgan D, Gordon MN, Holcomb L, Refolo L, Zenk B, Hardy J, Younkin S: Increased amyloid-β42(43) in brains of mice expressing mutant presenilin 1. Nature 1996, 383:710–713

53. Holcomb LA, Gordon MN, Jantzen P, Hsiao K, Duff K, Morgan D: Behavioral changes in transgenic mice expressing both amyloid precursor protein and presenilin-1 mutations: lack of association with amyloid deposits. Behav Genet 1999, 29:177–185

54. Wengenack TM, Whelan S, Curran GL, Duff KE, Poduslo JF: Quantitative histological analysis of amyloid deposition in Alzheimer's double transgenic mouse brain. Neuroscience 2000, 101:939–944

55. McGowan E, Sanders S, Iwatsubo T, Takeuchi A, Saido T, Zehr C, Yu X, Uljon S, Wang R, Mann D, Dickson D, Duff K: Amyloid phenotype characterization of transgenic mice overexpressing both mutant amyloid precursor protein and mutant presenilin 1 transgenes. Neurobiol Dis 1999, 6:231–244

56. Sadowski M, Wisniewski HM, Jakubowska-Sadowska K, Tarnawski M, Lazarewicz JW, Mossakowski MJ: Pattern of neuronal loss in the rat hippocampus following experimental cardiac arrest-induced ischemia. J Neurol Sci 1999, 168:13–20

57. Kim KS, Miller DL, Sapienza VJ, Chen CMJ, Bai C, Grundke-Iqbal I, Currie J, Wisniewski HM: Production and characterization of monoclonal antibodies reactive to synthetic cerebrovascular amyloid peptide. Neurosci Res Commun 1988, 2:121–130

58. Wisniewski HM, Sadowski M, Jakubowska-Sadowska K, Tarnawski M, Wegiel J: Diffuse, lake-like amyloid-β deposits in the parvopyramidal layer of the presubiculum in Alzheimer disease. J Neuropathol Exp Neurol 1998, 57:674–683

59. West MJ, Gundersen HJG: Unbiased stereological estimation of the number of neurons in the human hippocampus. J Comp Neurol 1990, 296:1–22

60. West MJ, Slomianka L, Gundersen HJG: Unbiased stereological estimation of the total number of neurons in the subdivisions of the rat hippocampus using the optical fractionator. Anat Rec 1991, 231:482–497

61. Gundersen HJG, Bendtsen TF, Korbo L, Marcussen N, Moller A, Nielsen K, Nyengaard JR, Pakkenberg B, Sorensen FB, Vesterby A, West MJ: Some new, simple and efficient stereological methods and their use in pathological research and diagnosis: review article. APMIS 1988, 96:379–394

62. Sadowski M, Wen PH, Elder GA, Robakis NK, Wisniewski T: Effect of the presenilin 1 P117L FAD linked mutation on hippocampal morphology transgenic mice. J Neuropathol Exp Neurol 2001, 60:543

63. Wadghiri YZ, Sigurdsson EM, Sadowski M, Li Y, Pappolla MA, Duff K, Turnbull D, Wisniewski T: Detection of Alzheimer's amyloid lesions in transgenic mice by magnetic resonance imaging. Magn Reson Med 2003, 50:293–302

64. Jimenez-Huete A, Alfonso P, Soto C, Albar JP, Rabano A, Ghiso J, Frangione B: Antibodies directed to the carboxyl terminus of amyloid β-peptide recognize sequence epitopes and distinct immunoreactive deposits in Alzheimer's disease brain. Alzheimers Rep 1998, 1:41–47

65. Wisniewski T, Frangione B: Apolipoprotein E: a pathological chaperone protein in patients with cerebral and systemic amyloid. Neurosci Lett 1992, 135:235–238

66. Tokuda T, Calero M, Matsubara E, Vidal R, Kumar A, Permanne B, Zlokovic BV, Smith JD, LaDu MJ, Rostagno A, Frangione B, Ghiso J: Lipidation of apolipoprotein E influences its isoform-specific interaction with Alzheimer's amyloid β peptides. Biochem J 2000, 348:359–365

67. Poduslo JF, Curran GL, Sanyal B, Selkoe DJ: Receptor-mediated transport of human amyloid β-protein 1–40 and 1–42 at the blood-brain barrier. Neurobiol Dis 1999, 6:190–199

68. Mirra SS, Gearing M, Nash F: Neuropathologic assessment of Alzheimer's disease. Neurology 1997, 49:S14–S16

69. Bales KR, Verina T, Cummins DJ, Du Y, Dodel RC, Saura J, Fishman CE, DeLong CA, Piccardo P, Petegnief V, Ghetti B, Paul SM: Apolipoprotein E is essential for amyloid deposition in the APPV717F transgenic mouse model of Alzheimer's disease. Proc Natl Acad Sci USA 1999, 96:15233–15238

70. Holtzman DM, Bales KR, Wu S, Bhat P, Parsadanian M, Fagan AM, Chang LK, Sun Y, Paul SM: Expression of human apolipoprotein E reduces amyloid-β deposition in a mouse model of Alzheimer's disease. J Clin Invest 1999, 103:R15–R21

71. Holtzman DM, Bales KR, Tenkova T, Fagan AM, Parsadanian M, Sartorius LJ, Mackey B, Olney J, McKeel D, Wozniak D, Paul SM: Apolipoprotein E isoform-dependent amyloid deposition and neuritic degeneration in a mouse model of Alzheimer's disease. Proc Natl Acad Sci USA 2000, 97:2892–2897

72. Maggio JE, Stimson ER, Ghilardi JR, Allen CJ, Dahl CE, Whitcomb DC, Vigna SR, Vinters HV, Labenski ME, Mantyh PW: Reversible in vitro growth of Alzheimer disease β-amyloid plaques by deposition of labeled amyloid peptide. Proc Natl Acad Sci USA 1992, 89:5462–5466

73. Christie RH, Bacskai BJ, Zipfel WR, Williams RM, Kajdasz ST, Webb WW, Hyman BT: Growth arrest of individual senile plaques in a model of Alzheimer's disease observed by in vivo multiphoton microscopy. J Neurosci 2001, 21:858–864

74. Wisniewski T, Lalowski M, Golabek AA, Vogel T, Frangione B: Is Alzheimer's disease an apolipoprotein E amyloidosis? Lancet 1995, 345:956–958

75. Shibata M, Yamada S, Kumar S, Calero M, Bading J, Frangione B, Holtzman D, Miller CA, Strickland DK, Ghiso J, Zlokovic, B. Clearance of Alzheimer's amyloid-$β_{1–40}$ peptide from brain by LDL receptor-related protein-1 at the blood-brain barrier. J Clin Invest 2000, 106:1489–1499

76. Zlokovic BV: Cerebrovascular transport of Alzheimer's amyloid β and apolipoproteins J and E: possible anti-amyloidogenic role of the blood-brain barrier. Life Sci 1996, 59:1483–1497

77. Ji Y, Permanne B, Sigurdsson EM, Holtzman DM, Wisniewski T: Amyloid β40/42 clearance across the blood-brain barrier following intra-ventricular injections in wild-type, apoE knock-out and human apoE3 or E4 expressing transgenic mice. J Alzheimer Dis 2001, 3:23–30

78. DeMattos RB, O'Dell M, Taylor JW, Parsadanian M, Bales KR, Paul SM, Holtzman DM: Early and marked increase in a-β deposition in PDAPP mice in the absence of both apoe and clusterin: evidence for a cooperative role in a-β clearance in vivo. 2003 Abstract Viewer/Itinerary Planner. Washington, DC, Society for Neuroscience, 2003, Program No. 666.14

79. Schenk D, Barbour R, Dunn W, Gordon G, Grajeda H, Guido T, Hu K, Huang J, Johnson-Wood K, Khan K, Kholodenko D, Lee M, Liao Z, Lieberburg I, Motter R, Mutter L, Soriano F, Shopp G, Vasquez N, Vandevert C, Walker S, Wogulis M, Yednock T, Games D, Seubert P: Immunization with amyloid-β attenuates Alzheimer disease-like pathology in the PDAPP mouse. Nature 1999, 400:173–177

80. Morgan D, Diamond DM, Gottschall PE, Ugen KE, Dickey C, Hardy J, Duff K, Jantzen P, DiCarlo G, Wilcock D, Connor K, Hatcher J, Hope C, Gordon M, Arendash GW: Aβ peptide vaccination prevents memory loss in an animal model of Alzheimer's disease. Nature 2001, 408:982–985

81. Weiner HL, Lemere CA, Maron R, Spooner ET, Grenfell TJ, Mori C, Issazadeh S, Hancock WW, Selkoe D: Nasal administration of amyloid-β peptide decreases cerebral amyloid burden in a mouse model of Alzheimer's disease. Ann Neurol 2000, 48:567–579

82. Greenberg SM, Bacskai BJ, Hyman BT: Alzheimer disease's double-edged vaccine. Nat Med 2003, 9:389–390

83. Doerfler P, Shearman MS, Perlmutter RM: Presenilin-dependent γ-secretase activity modulates thymocyte development. Proc Natl Acad Sci USA 2001, 98:9312–9317

84. Figueroa DJ, Morris JA, Ma L, Kandpal G, Chen E, Li YM, Austin CP: Presenilin-dependent γ-secretase activity modulates neurite outgrowth. Neurobiol Dis 2002, 9:49–60

85. Hadland BK, Manley NR, Su DM, Longmore GD, Moore CL, Wolfe MS, Schroeter EH, Kopan R: γ-secretase inhibitors repress thymocyte development. Proc Natl Acad Sci USA 2001, 98:7487–7491

86. Geling A, Steiner H, Willem M, Bally-Cuif L, Haass C: A γ-secretase inhibitor blocks Notch signaling in vivo and causes a severe neurogenic phenotype in zebrafish. EMBO Rep 2002, 3:688–694

87. Schenk D, Barbour R, Dunn W, Gordon G, Grajeda H, Guido T, Hu K, Huang J, Johnson-Wood K, Khan K, Kholodenko D, Lee M, Liao Z, Lieberburg I, Motter R, Mutter L, Soriano F, Shopp G, Vasquez N, Vandevert C, Walker S, Wogulis M, Yednock T, Games D, Seubert P: Immunization with amyloid-β attenuates Alzheimer disease-like pathology in the PDAPP mice. Nature 1999, 400:173–177

88. Lanz TA, Himes CS, Pallante G, Adams L, Yamazaki S, Amore B, Merchant KM: The γ-secretase inhibitor N-[N-(3,5-difluorophenacetyl)-L-alanyl]-S-phenylglycine t-butyl ester reduces A beta levels in vivo in plasma and cerebrospinal fluid in young (plaque-free) and aged (plaque-bearing) Tg2576 mice. J Pharmacol Exp Ther 2003, 305:864–871